Considerations of failure mechanisms associated with rock slope instability and consequences for stability analysis

by T.R. Stacey*

Synopsis

The results of a series of physical model studies of the stability of jointed rock slopes carried out some years ago are described. These models were tested under centrifugal loading. Four 'geological' structures were tested; all had the same joint orientations and strengths, but the relative spacing of the joints was different. The results showed that the mechanisms of failure of the slopes varied for the different models, and the gravitational loads at which failure developed also varied. The following conclusions are drawn from the results of the physical model tests:

- **the mechanism of slope failure is by progressive deformations throughout the slope**
- **the ratio of the spacings between the different sets of discontinuities exerts considerable influence on the slope failure**
- **in the models tested, the intact material strength had no noticeable influence on the stability of the jointed rock slopes (note that for hard rock, similitude conditions indicate a prototype slope height of 300 to 400 m, and therefore intact rock failure might not be expected under simple gravity conditions, i.e. no tectonic stresses)**
- **rock slope failures are three-dimensional and in general are not amenable to two-dimensional simplification**
- **knowledge of the orientations of discontinuities in the slopes does not allow prediction of a unique failure surface, nor of a volume of failure. The volume of failure is determined to a large extent by the plan configuration of the slope.**

Introduction

A very important study into failure mechanisms for high slopes in hard rock was carried out by Sjoberg (2000), in which he simulated five different mechanisms. Possibly the most important statement to come of out this work appears in his conclusions, 'There are, without a doubt, many other possible mechanisms, and there is also the possibility that these currently unknown (or poorly investigated) mechanisms are crucial for higher and steeper slopes than those presently existing.' A common approach to the interpretation of rock slope failure behaviour is to back-analyse failures from observations before and after the event. In such case studies, the interpretation of the 'failure surface' will usually be based on the observations after the event. In some cases there may be additional information from displacement monitoring data. Analyses will usually assume that failure takes place along that interpreted failure surface (or along a fictitious surface in a limit equilibrium analysis using a slip circle approach). A forward analysis of stability, or a slope design, will take into account orientations of geological planes of weakness to interpret potentially unstable wedge geometries, or development of failure in the rock mass. Back analyses will usually make use of a limit equilibrium approach, which considers the disturbing and resisting forces acting on the rock mass above the failure surface. Similarly, most forward stability analyses will then consider the stability of such wedges or potentially unstable masses along the interpreted failure surfaces. Questions that arise in this approach are:

- Is the chosen failure surface the surface on which failure actually took place?
- Are the back-analysed strength parameters of this surface representative of the 'strength' of the rock slope?
- Is the chosen failure surface a unique failure surface or does failure take place on more than one such surface?
- Does failure take place on multiple failure surfaces and in multiple locations within the slope?
- What about the three-dimensional geometry of the failure?

A programme of physical model tests, carried out on two- and three-dimensional models of jointed rock slopes, is described in this paper and provides some responses to these questions. These models were small

* *School of Mining Engineering, University of the Witwatersrand, South Africa.*

 SA ISSN 0038–223X/3.00 + 0.00. Paper received Apr. 2006; revised paper received May 2006.

scale models, and they were tested in a centrifuge to achieve the required levels of gravitational loading. The geometry, construction and testing of these models are discussed in the following sections.

Geometry of the models

Many failures of rock slopes appear to occur by sliding along major individual discontinuities such as fault planes and bedding planes, or along combinations of these planes. Before failure of the slope, it is often possible to recognize these potential failure planes, and apparently appropriate methods of slope stability analysis exist (for example, early publications by Londe *et al.*, 1969; John, 1968; Wittke, 1968; Hoek and Bray, 1981; and, more recently, Chen, 1995) that can be applied to such cases. However, do large slope failures actually occur as a result of such planar failures?

In addition, there are many rock slopes in which the configuration of discontinuities in the rock mass does not define a unique failure surface or combination of rock failure surfaces. Such a configuration is the very common and typical sedimentary rock mass—continuous bedding planes, a joint set continuous between the bedding planes and a further, discontinuous, joint set—where the angle of inclination of the bedding planes is less than both slope angle and angle of friction of the bedding plane surfaces. The potential 'failure surface' in this case is non-trivial. In this paper, investigations into the behaviour of rock slopes with this structural configuration, using small scale models, are described. The centrifugal test method was employed to test small scale two-and three-dimensional models. The configuration of the two-dimensional models is shown in Figure 1; the dip of the bedding planes was 33° and the dip of the cross joints 57°. Note that, with this model geometry, it was also possible to examine the behaviour of slopes in which the bedding dips into the slope—the left-hand slope in Figure 1.

The aims of the model tests were:

- to investigate qualitatively the progressive mechanisms of failure in rock slopes with the structural configuration described above
- to compare the behaviour of two-and three-dimensional slopes.

Although the discontinuity orientations were the same in all two-dimensional models, different ratios of joint plane spacings to bedding plane spacings were used. Four such ratios were tested, as summarized in Table I.

Properties of the model material and construction of the models

The physical models were constructed from an equivalent model material, which was developed as a similar material to quartzite (Krauland, 1971). It is therefore representative of a hard, brittle rock. The testing of the model material and the shear strength of the discontinuity surfaces is described in the following section. Thereafter, the preparation and testing of the models will be described.

Deformation and strength testing of the model material and the discontinuity

Uniaxial compression tests were carried out to determine the deformation properties of the intact model material. Cores were drilled from blocks of the model material for this purpose. These results are summarized in Table II for information.

Shear tests were carried out on specially prepared specimens: for the bedding planes, 54.8 mm diameter specimens were cored out of blocks of the model material. The cores were cut into discs that were subsequently ground to a thickness of 12.7 mm to produce 'bedding plane surfaces'. These discs were mounted in special holders and the shear strength of the surfaces tested in a Wykeham Farrance shearbox. Figure 2 shows a typical shear force-shear displacement curve for these surfaces. This shows that initial shear movements occur at low shear stress and that the shear strength increases with displacement to a residual value. The results of all bedding plane shear tests are shown in Figure 3. It was assumed that the saw cut joint surfaces would have the same shear properties as the bedding planes.

Specimens containing artificial joint surfaces were prepared such that the dimensions of the surface on which shear took place were 51 mm x 6.4 mm, with shear taking place across the 6.4 mm direction. Again tests were carried

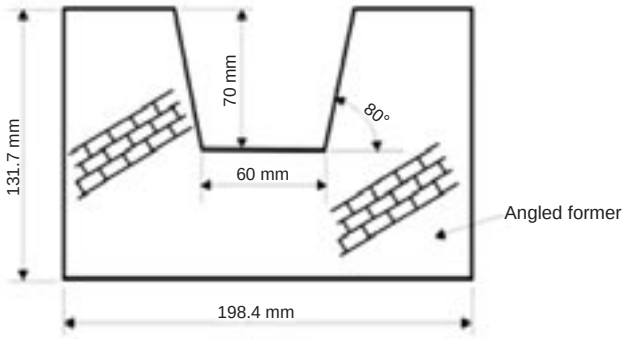

Figure 1—Configuration of two-dimensional models

Table I

Spacing of joints and bedding planes in the models

Bedding plane Spacing (mm)	Joints spacing (mm)	Spacing ratio	Number of models
3.4	12.7	3.74	4
4.6	12.7	2.76	5
3.4	6.35	1.87	4
6.35	6.35	1.0	5
3.4	12.7	3.74	3*

*Three-dimensional models

Table II

Deformation and strength properties of intact model material

Data	Modulus of elasticity (GPa)	Poisson's ratio	Uniaxial compressive strength (MPa)
Mean	4.2	0.18	3.9
Std deviation (%)	11	15	16
Number of specimens	13	13	45

out in the shear box, with the specimens being mounted in a specially prepared holder. The results of these tests are shown in Figure 4. Only the peak shear strength was tested since the bedding plane tests yielded the residual shear strength of the material.

Preparation of the physical models

The model material was prepared in the form of blocks, which were subsequently cut into thin plates. The plates were ground on both sides using a tombstone grinding machine. These ground surfaces represented the bedding plane surfaces. The thin plates were cut into strips 12.7 mm wide. In the three-dimensional models, the sides of the strips represented the continuous set of joints between bedding planes. Their width represented the spacing of this joint set. Cross joints at right angles to the bedding planes and to the continuous joints were formed in the strips by inducing tensile fractures across the thickness of the strips. The spacing of these induced joints was 12.7 mm for the three-dimensional models, but variable, as in Table I above, for the two-dimensional models.

In all models the slope angle was 80° and the slope height was 70 mm.

The two-dimensional models were built up by hand using strips of model material 12.7 mm wide, in which artificial joints had been induced. The pieces of model material comprising the strips were placed so that joints were continuous between two bedding planes only, that is, they were staggered so that joint planes in one strip did not coincide with joint planes in adjacent strips. The continuity of this joint 'set' was therefore 50%. An angled former, placed in the corner of the model supporting frame, determined the inclination of the bedding planes. In the first two models an angle of 30° was used. However, with this bedding plane dip no slope failures occurred and therefore all subsequent models were built with the bedding dipping at an angle of 33°. Joint spacing and bedding spacing were constant throughout a model.

Three three-dimensional models were prepared and their toe plan configurations are shown in Figure 5. Note that, in models 2 and 3, the radius of curvature given applies to the central 90° arc and that the remaining curvature has a smaller radius, that is, there is a compound curvature. The models were built up by hand from the base using the 12.7 mm wide jointed strips. A bedding plane dip of 33° was used and the strips were laid at an angle of 45° to the central vertical section through the pit. The resulting geological structure is summarized in Table III in which it is assumed that north is the direction of the radius arrows in Figure 5.

This geological structure allowed for sliding on the bedding planes, with the two joint sets providing release planes.

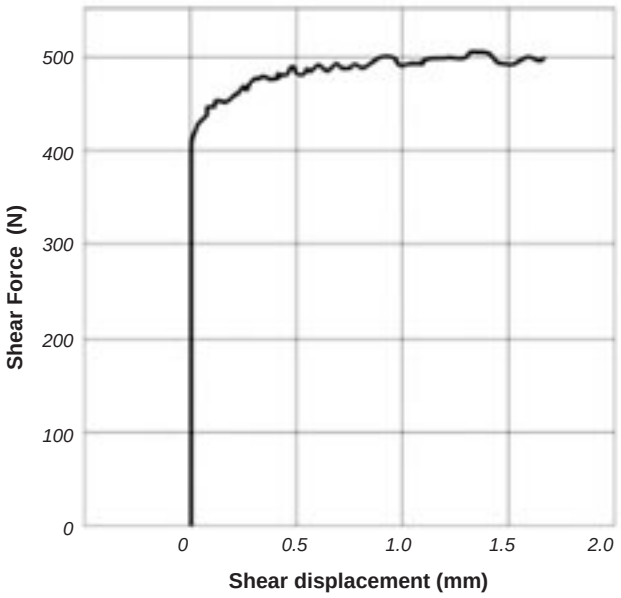

Figure 2—Typical shear force-shear displacement curve for 'bedding plane' surfaces

Testing of the physical models

The models were tested in a large centrifuge (described by Hoek, 1965), capable of imposing a simulated gravitational acceleration of up to 1000 g. Physical model testing in a centrifuge is common in the civil engineering environment

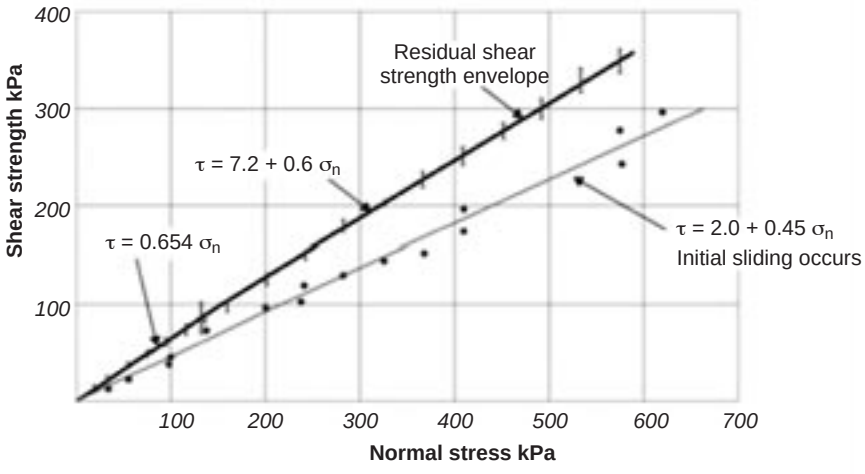

Figure 3—Results of bedding plane shear tests

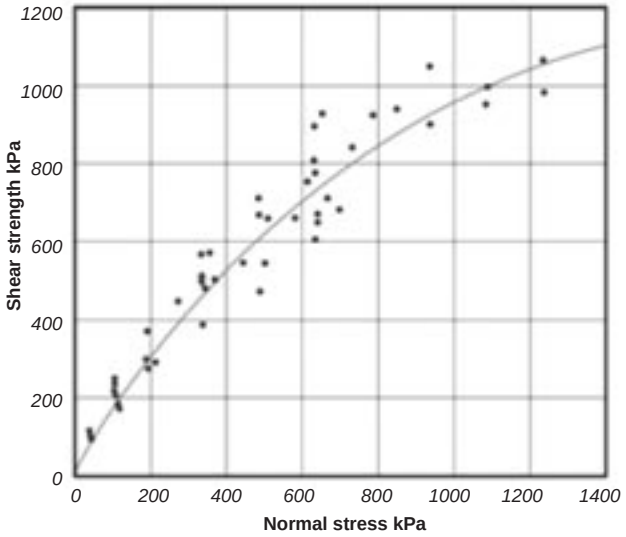

Figure 4—Results of shear tests on artificial joints

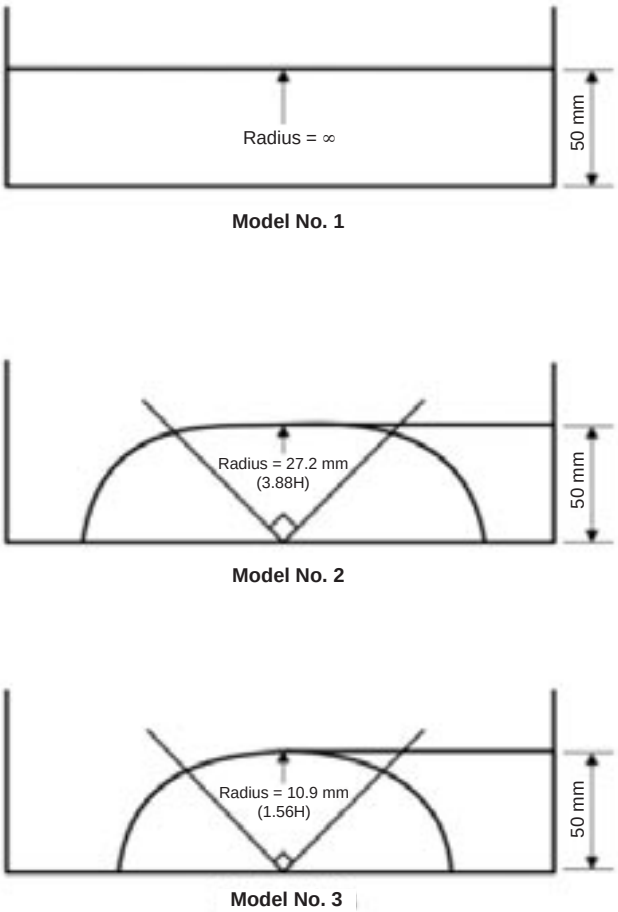

Figure 5—Floor plan configurations of the three-dimensional models

(for example, Phillips *et al.*, 2002), but it has apparently not been used recently for deep, hard rock situations. In the testing programme, there was no intention to simulate a particular prototype slope, but simply to investigate slope behaviour mechanisms. Therefore, the testing procedure involved gradually increasing the centrifugal loading until maximum values of about 600 g and 550 g were attained for the two- and three-dimensional models, respectively. For interest, at the maximum gravitational loading, the height of a similar (prototype) slope in hard rock would be in the 450 m to 500 m range. Model behaviour during centrifugal loading was recorded photographically using a triggered stroboscope as a light source.

Figures 6, 7, 8 and 9 show examples of typical sequences of failure of the two-dimensional models (the numbers of models tested are given in Table I). It is immediately apparent from these figures that failure takes place by progressive sliding on the bedding planes, generally throughout the height of the slope, with tensile opening of the cross joints. Rotation of blocks was also observed, particularly in the case of the 1:1 joint to bedding plane spacing. Failures are therefore combinations of different mechanisms. Stepped 'surfaces' are formed that have average angles of inclination that are much steeper than the dip of the bedding planes. A slight bulging of the slope face just above the toe was noticed before failure in some of the models. This was apparently due to sliding on the bedding planes in this region. The intact strength of the material had no apparent effect on the failure of the slope since no failures of intact pieces were observed before a collapse. However, the small pieces that were involved in the collapse debris were found to be crushed and broken up to some extent. After collapse, the presence of the collapse debris at the base of the slope generally had a stabilizing effect on the remaining slope.

The mode of failure of the model slopes appeared to be controlled entirely by the ratio of the joint spacing to the bedding plane spacing. This in turn controls the capacity of the configuration to transmit tensile stress and also the amount of sliding which can take place in the 'coherent' mass before complete separation of adjacent pieces occurs, resulting in collapse. This can be easily understood by referring to Figure 10. In this figure are shown two small sections of a rock mass consisting of continuous bedding planes and discontinuous cross-joints. In the two cases the joints have different spacings. If there is a compressive stress acting normal to the bedding planes, then, by virtue of the shear strength of the bedding planes, a tensile stress can be sustained in a direction normal to the joint planes. The magnitude of this tensile strength is dependent on the spacing of the joints i.e. the length 'd'. It is clear, therefore, that, in the first case where the joint spacing is small, the capacity to withstand tensile stress will be much lower than in the second case where joint spacing is greater. It is clear also that more sliding can take place in the second case before complete separation occurs and a tension crack is formed.

As can be seen from Table I, four different values of the ratio of joint spacing to bedding plane spacing were tested in the two-dimensional models. The modes of failure will now be considered for each ratio in turn.

Joint spacing to bedding plane spacing ratio S = 1.0 (Figure 6)

There is very little displacement along the bedding planes of the right-hand slope before collapse of some material occurs

Table III

Geological structure of the three-dimensional models

Discontinuity plane	Strike (degrees)	Dip (degrees)	Spacing (mm)	Continuity	Discontinuity surfaces
Bedding	N90°E	33°S	3.4	Continuous	Ground faces of the strips
Joint	N51°W	67.5°NE	12.7	Continuous between, but not across bedding	Diamond saw cut edges of the strips
Joint	N51°E	67.5°NW	12.7	Discontinuous	Artificial joints induced by tensile fracture

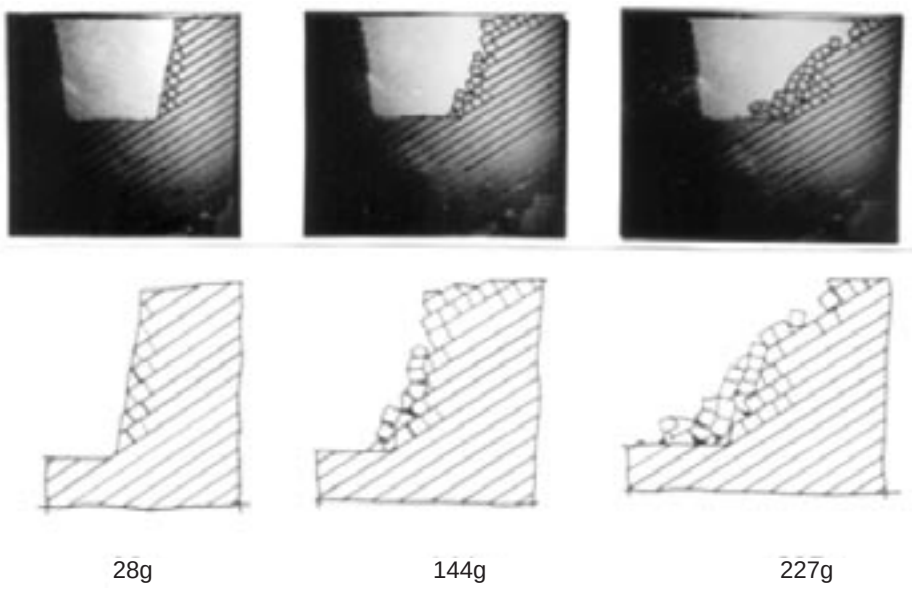

Figure 6—Two-dimensional model (S = 1.0)

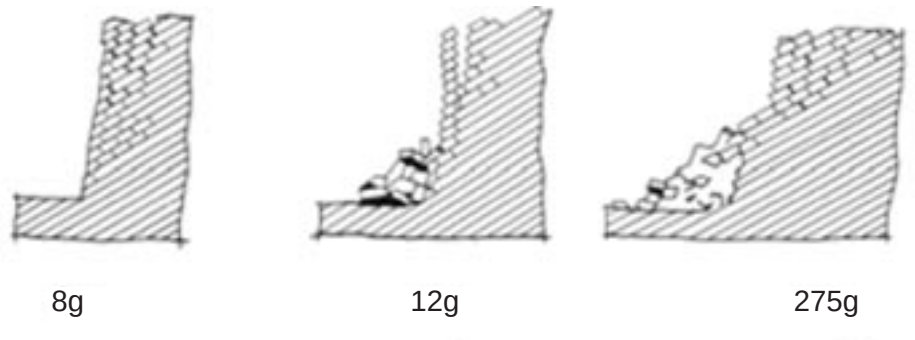

Figure 7—Two-dimensional model (S = 1.87)

indicating that very little tensile stress can be sustained in a direction parallel to the bedding planes. Consequently, no tension cracks (or only very small ones) were formed behind the crest of the slope. Therefore, a geological configuration such as in these models would give very little warning of an impending slope failure.

With increasing centrifugal acceleration, the right-hand slope breaks back further, additional collapses again occurring with little warning. Rotational movements of some of the pieces of material occurred in several cases.

This configuration, with S = 1.0, was the only one in which any failure of the left-hand slope occurred, as can be seen in Figure 6. Rotational movements of the blocks occurred and this type of failure may be ascribed to toppling.

Joint spacing to bedding plane spacing ratio S = 1.87 (Figure 7)

The behaviour of the right-hand slopes with this configuration was characterized by the opening up of joints close to the face of the slope at very low centrifugal accelerations, owing to sliding on the bedding planes. This sliding occurs over the whole height of the slope. Failure progresses by the increased opening of joints further back into the slope. Further sliding occurs on the bedding planes and stacked columns of material pieces are formed, which can stand entirely free from contact with the rest of the slope. These columns eventually become unstable when displacements on the bedding planes become too great, and collapse finally

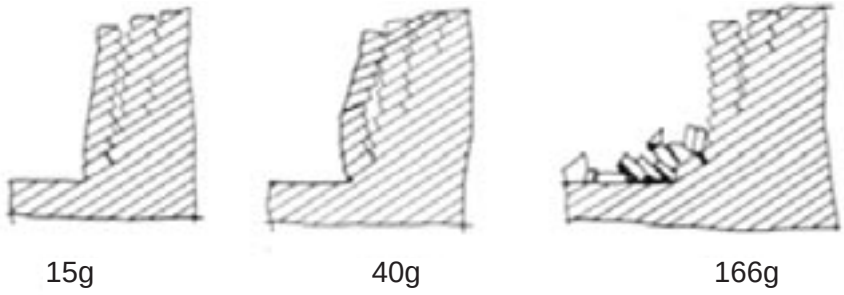

Figure 8—Two-dimensional model (S = 2.76)

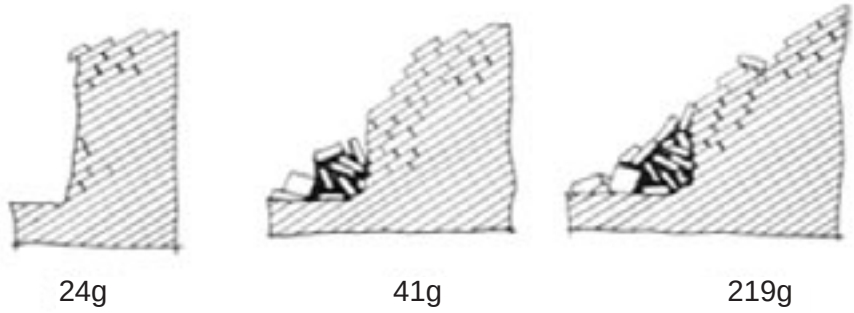

Figure 9—Two-dimensional model (S = 3.74)

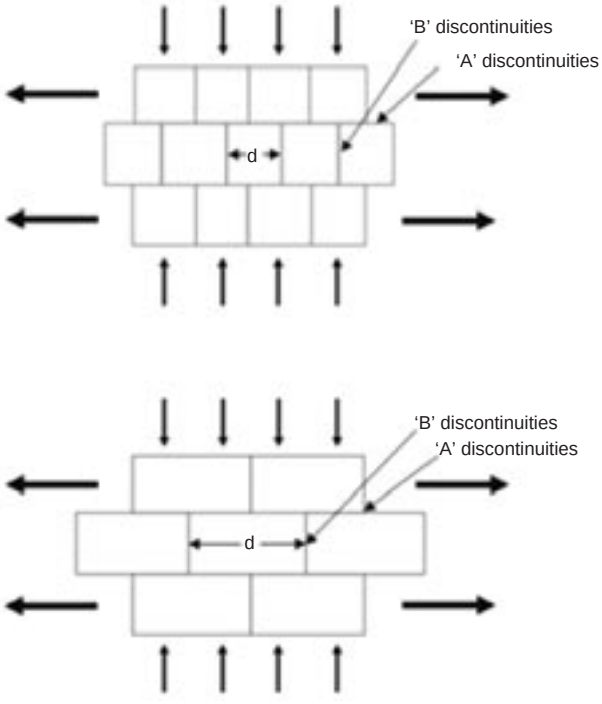

Figure 10—Effective tensile strength of rock mass

occurs. Failure progresses backwards into the slopes, and, as each column collapses, a larger pile of rubble is formed, stabilizing the lower parts of the slope.

Joint spacing to bedding plane spacing ratio S = 2.76 (Figure 8)

Similar behaviour to that for S = 1.87 was observed. Sliding on the bedding planes again took place over the whole height of the slope and column formation was again evident, very deep tension cracks being produced. The columns in this case were more stable, however, owing to their greater base width. Figure 8 shows an interesting case—a column became detached complete over most of the slope height, then began to buckle and, in so doing, the top of the column again made contact with the rest of the slope. This stabilized the bulging column for some time before it finally collapsed.

The stable loosening of the mass behind the crest of the slope is increased in extent compared with S = 1.87 (Figure 7).

Joint spacing to bedding plane spacing ratio S = 3.74 (Figure 9)

Very large displacements along the bedding planes before collapse characterize the behaviour in this case. Consequent opening up of joints far behind the crest of the slope occurs. This behaviour is due to the capacity of the mass to withstand a considerable degree of tensile stress in the direction parallel to the bedding planes. The slope even reached the overhanging stage before final collapse took place. Collapse involved only the upper half of the slope.

Discussion

Although the behaviour of models with the same S value was similar, there was some variation in the centrifugal acceleration at which corresponding deformations, and collapse, occurred for models with this S value. It is believed that the main reason for this is the variation in the placing of the pieces of model material. Referring to Figure 11, it can be seen that the same joint spacing, but different relative location, will yield different tensile strengths normal to the joint plane. If a slope has the relative joint location shown in

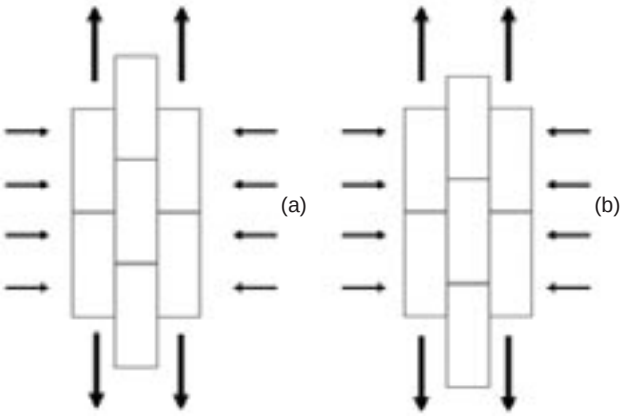

Figure 11—Influence of joint location on rock mass tensile strength

case (b) then joints will open more easily than if case (a) occurs. Consequently the case (b) type slope will fail sooner. In building up the models it was attempted to adhere to case (a) joint geometry. However, small variations occurred and probably explain the differences in the failure accelerations of the models. Recent numerical modelling using a discrete element method (Salim and Stacey, 2006) has shown behaviour similar to that observed in the physical models with regard to the locations of failure, the progressive development of failure and the influence of the relative locations of the joints.

The mode of failure of all model slopes tested was progressive. Failure of the right-hand slope was by progressive sliding down along bedding planes. In no case did collapse of the entire slope occur without warning. There was no clearly defined single surface of failure, and these slopes would therefore not be amenable to conventional slope stability analysis by limit equilibrium methods. Failure of the left hand slope only occurred with S = 1.0.

The proximity of the boundaries showed no obvious influence on the behaviour of the models.

Three-dimensional models

As with the two-dimensional models, failure took place by sliding on the bedding planes, and there was evidence of opening up of joints. Since the models were three-dimensional and slopes under load in the centrifuge were photographed from the front (i.e. the slope faces were photographed), it was not possible to study the progressive opening of joints. The progressive nature of failure was only apparent by sequential sliding of pieces of material from the face of the slope. The quality of the photographs taken during centrifugal loading is not satisfactory for reproduction in this paper.

Figures 12a, 12b and 12c show the extent and volume of failure in the three dimensional models. These photographs also illustrate the geological structure modelled.

The model with a plane slope displayed a break-back much greater than the other 3D models. These models were bounded laterally by the sides of the box containing the model, which effectively formed 'large lateral faults' along which the rock mass slope could fail, and, as a result of this side boundary effect, the plane slope failed along its whole strike length. The extent of failure was defined by the slope geometry and the dip of the bedding planes and is equivalent to the two-dimensional situation (Figure 9). When the plan radius of curvature of the slope becomes less than infinity, the volume of the failure is restricted considerably (Figures 12a and 12b). The presence of the cross-joints allows a

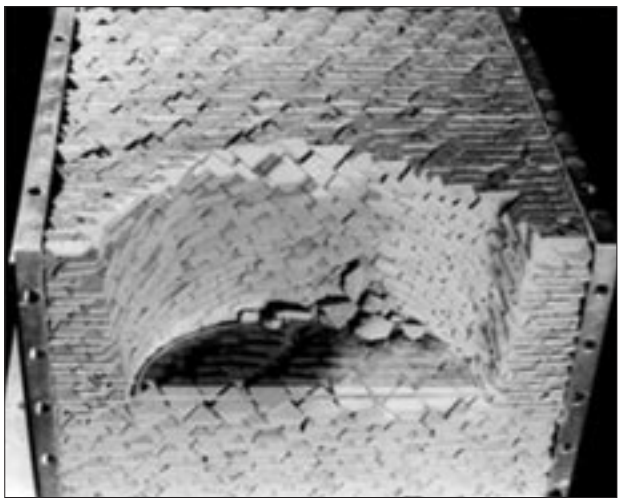

Figure 12a—Model with normalized floor plan radius of curvature of 1.56

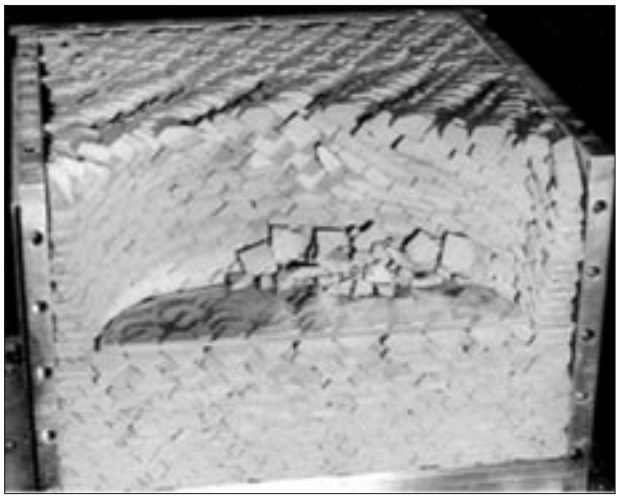

Figure 12b—Model with normalized floor plan radius of curvature of 3.88

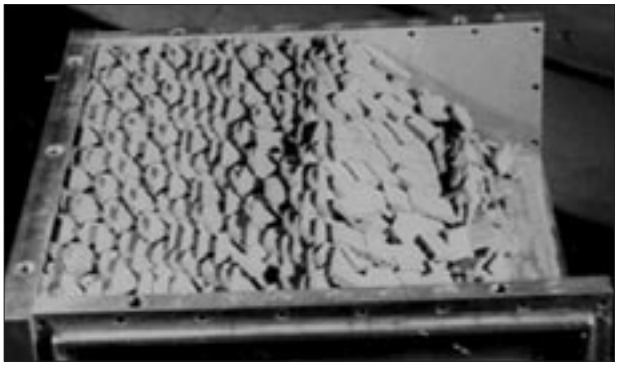

Figure 12c—Model with floor plan radius of curvature of ∞

Table IV

Break-back results for the three- and two-dimensional models

Normalized radius of curvature (Toe radius/slope height)	Break-back (mm)
∞	33
1.56	8
3.88	18
∞ (2D models)	30–34

'wedge' of material to slide out on the bedding planes with associated opening of the joints. The configuration of the failed zone becomes fully three-dimensional and cannot be idealized by a two-dimensional cross-section. The break-back of the slope is much restricted for smaller plan radii of curvature and approximate quantitative distances of break-back are summarized in Table IV for the three- and two-dimensional models.

The variation in the distances of break-back indicates clearly the stabilizing effect of small plan radius of curvature. It is clear from Table IV that, even for large radii, the slope failure would still be restricted. Interpretation and extension of these results using a joint trace model (Armstrong and Stacey, 2005) indicates that the beneficial effects of concave curvature of the slope disappears at a normalized radius of curvature of about 10, as shown in Figure 13.

Piteau and Jennings (1970), in extrapolating empirical data on slopes in the Kimberley area, found that the effect of plan radius of curvature became negligible for radii only in the region of 20 times the slope height. Their results referred to the slope plan radius at surface, however, whereas the model results above refer to the plan radius at the toe of the slope.

The restriction of the failure also applied to the centrifugal acceleration at which the failure occurred. In the case of the plane slope, failure occurred in the same range of centrifugal accelerations as observed in the two-dimensional models. However, for the three-dimensional models with smaller plan radii of curvature, failure occurred only at higher centrifugal accelerations. The practical interpretation of this is that instability would develop only for greater slope heights.

Conclusions

The model tests have shown that, in the absence of clearly predefined failure surfaces, failure of a rock slope does not take place in the form of sliding of a coherent mass of material. The two-dimensional tests indicated that the failure is progressive, with deformations taking place throughout the slope. It is believed that, in real rock slopes, the development of failure very commonly involves this type of behaviour. In the particular configuration tested where bedding planes dipped towards the slope face, failure was by sliding on the bedding planes, with associated opening of cross-joints, and some rotation in the 1:1 joint to bedding plane spacing case. Slope failure involved a combination of two or three different mechanisms. The mechanism of the progressive slope failure and the form of the resulting surfaces of failure (note that an overall single failure surface, as applied in a limit equilibrium analysis, could not be defined) depended on the spacing, continuity and shear strength of the planes of weaknesses and on the ratio between the spacings of different sets of these planes (i.e. ratio of joint spacing to bedding plane spacing). It was the value of this ratio that appeared to determine the form of the slope failure. The smaller the ratio, the less the tensile stress that can be sustained by the mass and the greater the likelihood of toppling of rock blocks. Essentially, except for the spacings of joints, in which only

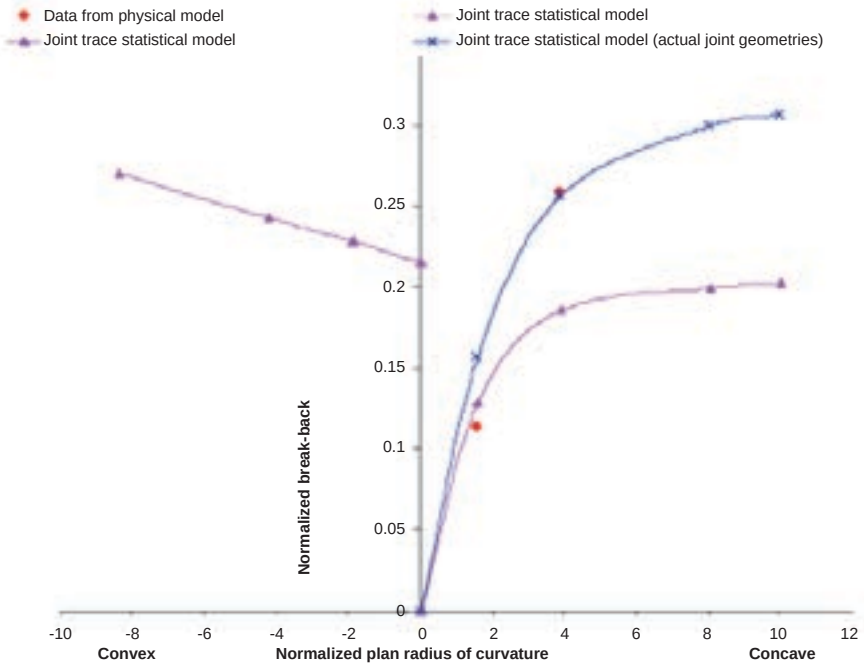

Figure 13—Break-back as a function of slope plan radius of curvature

the mean values varied, all jointing parameters (geometry and strength) were identical in all the models. However, the behaviour mechanisms of the models were significantly different. In the configuration where bedding planes dipped into the slope face, slope failures were found to occur only for the smallest value of the joint spacing to bedding plane spacing ratio tested, namely S = 1.0. Based on the variations in observed slope behaviour, it may be concluded that prediction of the behaviour of real rock slopes using deterministic analyses is unlikely to be successful, and that probabilistic approaches, taking into account the jointing variability, will be required to provide realistic answers.

The three-dimensional tests proved that, for analysis of slope stability, it is in general not admissible to consider a two-dimensional section through the slope. The plane slope model (plan radius of curvature infinity) showed very similar behaviour to the equivalent two-dimensional models, indicating that, in this case, a two-dimensional simplification is justified. However, model slopes with a concave radius of curvature showed a great increase in stability, failures being truly three-dimensional in form and occurring only at higher centrifugal accelerations. The volumes of material involved in the failures were smaller for smaller plan radii of curvature. In real slopes, failure geometries are generally three-dimensional, even if the slope has a plane geometry.

The intact strength of the material had no apparent effect on the behaviour of the slopes. This is to be expected since the model material used simulated hard rock. Softer, weaker rocks would have an influence on the failure behaviour of slopes.

For the configuration of discontinuities and models tested, the following conclusions may be summarized:

- The mechanism of slope failure is by progressive deformations throughout the slope
- Slope failure involved a combination of two or three different mechanisms
- The ratio between the spacings of different sets of discontinuities exerts considerable influence on the slope failure
- Realistic prediction of real jointed rock slope behaviour is only likely to be possible using probabilistic approaches
- In the models tested, the intact material strength had no noticeable influence on the stability of jointed rock slopes
- Rock slope failures are usually three-dimensional and in general are not amenable to two-dimensional simplification
- Knowledge of the orientations of discontinuities in the slopes does not allow prediction of a unique failure surface nor of a volume of failure. The stability of a slope and, if failure does occur, the volume of the failure, are determined to a large extent by the plan configuration of the slope.

References

ARMSTRONG, R. and STACEY, T.R. (2005) The extent and volume of three dimensional failures in rock slopes in which several sets of joints define the geological structure, *Proc. 3rd Southern African Rock Engng Symp. Best practices in rock engineering*, Randburg, S. Afr. Inst. Min. Metall., Symposium Series S41, pp. 201–209.

CHEN, Z. Recent developments in slope stability analysis. *Proc. 8th Int. Cong. Int. Soc. Rock Mech.*, Tokyo, Balkema, vol. 3, 1995. pp. 1041–1048

HOEK, E. The design of a centrifuge for the simulation of gravitational force fields in mine models. *Jl S. Afr. Inst. Min. Metall.*, vol. 65, 1965. pp. 455–487.

HOEK, E. and BRAY, J.W. *Rock Slope Engineering*. 3rd Edition, E & FN SPON for The Institution of Mining and Metallurgy, London, 358 pP.

JOHN, K.W. Graphical stability analysis of slopes in jointed rock. J. Soil Mech. Fds Div. Am. Soc. Civ. Engrs, vol. 94, no. SM2, 1981. 1968. pp. 497–526.

KRAULAND, N. The behaviour of a prototype and a model mine tunnel, *The Technology and Potential of Tunnelling*, N. Cook, (ed.) Associated Scientific and Technical Societies of South Africa, 1971. pp. 135–140.

LONDE, P., VIGIER, G., and VORMERINGER, R. Stability of rock slopes, a three-dimensional study, *J. Soil Mech*. Fdns Div. Am. Soc. Civ. Engrs, vol. 95, no. SM1, 1969. pp. 235–262.

PHILLIPS, R., GUO, P., and POPESCU, R. *Physical Modelling in Geotechnics: ICPMG '02*, A.A. Balkema. 2002.

PITEAU, D.R. and JENNINGS, J.E.B. The effects of plan geometry on the stability of natural rock slopes in rock in the Kimberley area of South Africa. *Proc. 2nd Int. Cong. Int. Soc. Rock Mech.*, Belgrade, vol. 3, Theme 7, Paper no. 4. 1970.

SALIM, A. and STACET, T.R. Unstable rock slope behaviour in a discontinuous rock mass, *Proc. Symp. SANIRE 2006—Facing the Challenges*, Rustenburg, S. Afr. National Institute For Rock Engineering, paper in preparation. 2006.

SJOBERG, J. Failure mechanisms for high slopes in hard rock, *Slope Stability in Surface Mining*, Hustrulid, McCarter and Van Zyl (eds.), SME, Colorado, 2000. pp. 71–80.

STACEY, T.R. The behaviour of two-and three-dimensional model rock slopes. *Q. Jl. Engng Geol.*, vol. 8, 1974. pp. 67–72.

WITTKE, W. Standsicherheitsberechnung von Felsboeschungen, VDI Z, vol. 110, no 17, 1968. pp. 689–696. ◆